Dielectric Properties of Layered Silicate-Reinforced Natural and Polyurethane Rubber Nanocomposites

G. C. Psarras,[1] K. G. Gatos,[2] J. Karger-Kocsis[2]

[1]*Department of Materials Science, School of Natural Sciences, University of Patras, Patras 26504, Greece*
[2]*Institute for Composite Materials, Kaiserslautern University of Technology, Erwin Schrödinger Str., Kaiserslautern, D-67663, Germany*

Received 9 February 2007; accepted 13 May 2007
DOI 10.1002/app.26831
Published online 12 July 2007 in Wiley InterScience (www.interscience.wiley.com).

ABSTRACT: Natural rubber (NR), polyurethane rubber (PUR), and NR/PUR-based nanocomposites were prepared by adding a pristine synthetic layered silicate (LS; sodium fluorohectorite) in 10 parts per hundred parts rubber, following the latex compounding route. The dispersion of the LS latices in the composites was studied by means of X-ray diffraction (XRD) and transmission electron microscopy (TEM). The morphology-dependent dielectric properties of the produced nanocomposites were examined using broadband dielectric spectroscopy (BDS) at ambient temperature. Besides the glass/rubber transition of the polymer matrices, interfacial polarization (IP) is evident in the produced nanocomposites. The α-relaxation, as well as the β-mode, in the PUR-containing nanocomposites proved to be less affected by the presence of LSs. The obtained experimental data suggest that the LS is more compatible with and thus better intercalated by the PUR than by the NR which was prevulcanized in this case. © 2007 Wiley Periodicals, Inc. J Appl Polym Sci 106: 1405–1411, 2007

Key words: dielectric spectroscopy; nanotechnology; natural rubber; polyurethane; layered silicate

INTRODUCTION

Polymer-based nanocomposites contain nanometer size fillers usually in rather small amount. The physical, mechanical, and electrical properties of nanocomposites can be tailored by their preparation routes (incorporation of ''preformed'' particles or *in situ* production of the latter) and formulations (e.g., types and content of nanoinclusions). Nanocomposites can be used in diverging sectors as structural and functional materials (e.g., coatings, packaging to medical or biomedical products, electronic and photonic devices, dielectrics and electrical insulators, smart materials).[1,2] Rubber nanocomposites incorporating layered silicates (LSs) as reinforcement are attracting increased scientific and technological interest. This is due to the high reinforcing efficiency of the LS, even at very low loading. Note that the average thickness of LS is 1 nm and its aspect ratio (length to thickness ratio) may be as high as 2000 for some man-made LSs.[3–6] LSs in the polymer matrix usually attain intercalated and exfoliated structures. In the first structure, the polymer molecules are inserted between the silicate layers expanding the basal spacing, while in the second one individual silicate platelets are dispersed randomly in the polymer matrix.[3] In the present study, natural (NR) and polyurethane rubbers (PUR) as well as their blend are used as matrices for the production of a set of nanocomposites. Nanocomposites were prepared by adding a pristine synthetic LS (sodium fluorohectorite) in 10 parts per hundred parts rubber (phr), following the latex compounding route. The dispersion of the LS in the composites was studied using X-ray diffraction (XRD) and transmission electron microscopy (TEM). The morphology-dependent dielectric properties of the produced nanocomposites were examined by using broadband dielectric spectroscopy (BDS) at ambient temperature.

EXPERIMENTAL

Materials

As LS a synthetic sodium fluorohectorite (Somasif ME-100) from Co-op Chemicals (Tokyo, Japan) was selected. This LS had a cation exchange capacity of 100 meq/100 g and an intergallery distance of 0.95 nm. Note that this LS exhibits a very high aspect ratio, $\sim$ >1000. Sulfur prevulcanized NR latex was procured from the Rubber Research Institute of India (Kottayam, Kerala, India). This concentrated, high-ammonia (1%) NR latex contained 60% dry rubber. For prevulcanization, this latex was mixed with

Correspondence to: G. C. Psarras (G.C.Psarras@upatras.gr).
Contract grant sponsor: PPP IKYDA 2005 program, DAAD–IKY, Greek State Scholarships Foundation.

Journal of Applied Polymer Science, Vol. 106, 1405–1411 (2007)

sulfur and zinc dimethyl dithiocarbamate under slow stirring as described elsewhere.[5] The compounded latex was then heated to 70°C in a water bath with low stirring for 4 h. The prevulcanized latex obtained was cooled to room temperature and the initial ammonia content was restored by adding ammonia solution. The NR latex was then stored in tight plastic bottles until use. PUR latex (Impranil DLP-R) containing ~ 50% polyester-based polyurethane was supplied by Bayer AG (Leverkusen, Germany).

Film casting

The prevulcanized NR latex was mixed with the aqueous dispersion of LS (10%) and stirred well. The dirt and coarse particles were removed by filtering through a sieve (opening 250 μm) and the latex compound was cast in a mold build of glass plates (dimensions: 130 mm × 100 mm × 2 mm). The casting was allowed to dry in air till transparent and post vulcanized at 100°C for 30 min in an air circulated oven. Fully vulcanized samples were then cooled and packed in sealed polyethylene bags for testing. Aqueous dispersion of LS was added to the PUR latex stirred and cast as indicated above and air dried till transparent. Note that PUR has not been cured and the LS amount in the related composites was 10 phr.

Latex blends of PUR/NR with and without LS were produced in a similar way as described above.

Morphology detection

The dispersion of LS in the latex films was studied using XRD and TEM. XRD spectra were obtained in transmission mode using Ni-filtered CuK_α radiation ($\lambda = 0.1542$ nm) by a D500 diffractometer (Siemens, Munich, Germany). The samples were scanned in step mode by 1.5°/min rate in the range of $2\theta < 12°$. For comparison purpose, the XRD spectrum of the LS powder was also registered, however, in reflection.

Thermal characterization

A Diamond (Perkin–Elmer, Shelton, USA) differential scanning calorimeter operating at a scan rate of 10°C/min was used to characterize thermal transitions in pure and reinforced PUR, NR, and PUR/NR systems. Samples were placed in an aluminum crucible and an empty aluminum crucible served as reference. Temperature was varied from −80 to 60°C.

Dielectric response

Broadband dielectric measurements were performed in the frequency range of 10^{-3} to 10^{7} Hz, by means of Alpha-N Frequency Response Analyser (Novocontrol Technologies GmbH, Hundsangen, Germany) at RT (~20°C). The employed test cell was a two electrodes plate capacitor, BDS 1200 supplied also by Novocontrol, which was suitably shielded. Samples were placed between parallel electrodes without any surface treatment.

RESULTS AND DISCUSSION

Morphology

Morphology of polymer matrix/LS nanocomposites exhibit three different configurations: (a) microphase-separated composites, where polymer matrix and LSs remain immiscible; (b) intercalated structures, where polymer molecules are inserted between the silicate layers; and (c) exfoliated structures, where individual silicate layers are dispersed in the polymer matrix.[3,7,8] Furthermore, the coexistence of two or more configurations in a nanosystem cannot be excluded. XRD patterns and TEM images are the two most frequently used techniques for identifying the intercalation/exfoliation of LS in polymeric composites.[3,8] Results from the XRD spectra of the LS and the LS-containing films of various compositions are presented in Table I. The LS spectrum includes three peaks. According to Bragg's equation these peaks correspond to the following interlayer distances: 1.22, 1.10, and 0.96 nm; so, the LS used contained some small fractions with higher intergallery distance than the bulk material.[5] The intercalation of LS by NR, in the related compound, becomes evident since the interlayer distance of the LS increased to 1.19–1.31 nm. The position and shape of the related XRD peak suggested that the degree of NR intercalation is rather poor and various NR-intercalated LS populations exist.[5] Considerably better intercalation of LS has been achieved by the PUR latex. The relative XRD spectrum exhibits two well-separated peaks, where the major peak indicates that the interlayer distance of the LS widened to 1.73 nm from the initial 0.95 nm. This effect can be assigned to the higher polarity of PUR compared to NR, which favors the compatibility with LS.[5] The response of the reinforced blend (PUR/NR + 10 phr LS) includes also two peaks, corresponding at somehow higher interlayer distances with respect to those of PUR. The absence of the characteristic peak of LS in the XRD spectra of the nanocomposites has been used as a first hand indication for the exfoliation of the clay platelets.[8] However, as the XRD intensity at low angles and at partial exfoliation of the silicate is strongly reduced, the missing peak in the spectrum does not necessarily mean exfoliation. At this point the inspection of TEM images could provide useful information for the exfoliation or not of silicates. TEM

TABLE I
Peak Position and Interlayer Distance as Derived from the XRD Spectra of the LS-Reinforced Rubber Nanocomposites

	Peak position (2θ, °)	Interlayer distance (nm)
LS	7.25/8.04/9.31	0.95/1.10/1.22
NR + 10phr LS	6.75/7.43	1.19/1.31
PUR/NR + 10phr LS	4.23/6.75	1.31/2.09
PUR + 10phr LS	5.11/7.19	1.23/1.73

For comparison reason results from the XRD spectrum of LS are also included.[5]

images shown in Figure 1 give evidence for the good dispersion of LS, mostly in intercalated stacks, in PUR. The high aspect ratio of LS is clearly recognizable by considering some flat-on laying LS platelets.

The TEM pictures in Figure 2 show the dispersion of LS in the PUR/NR latex blend. Since, NR and PUR are not compatible (amplified by the prevulcanization of NR), and the intercalation of LS by NR is poor,[5] the LS stacks are preferentially located in the PUR phase.[5] The LS is mostly intercalated by PUR, but few exfoliated silicate platelets can also be found on the related TEM pictures. In a previous study,[5] it was shown that silicate layers and aggregates cover the NR particles, resulting in a skeleton (house of cards) structure. This peculiar morphology is rather specific for NR nanocomposites produced by the latex route if the length of the LS is commensurable with that of the rubber particle size in the latex.

Thermal analysis

Figure 3 shows the DSC thermographs of all the tested samples. In all cases a glass/rubber transition is recorded. In the heating traces of PUR/NR and PUR/NR + 10 phr LS samples, two distinct steps are present, corresponding to the glass transition of each polymer constituent. Glass transition temperatures were determined by using suitable software supplied by Perkin–Elmer, via the point of inflection of the transition (Table II).

Dielectric response

BDS has been proved to be a powerful tool for the investigation of molecular mobility, phase changes, conductivity mechanisms, and interfacial effects in polymers and complex systems.[9,10] Dielectric data can be analyzed by means of different formalisms such as dielectric permittivity mode or electric modulus mode. In the present study, all dielectric data and the related relaxation processes are investigated via the electric modulus formalism. Electric modulus is defined as the inverse quantity of complex permittivity by the following equation:

$$M^* = \frac{1}{\varepsilon^*} = \frac{1}{\varepsilon' - j\varepsilon''} = \frac{\varepsilon'}{\varepsilon'^2 + \varepsilon''^2} + j\frac{\varepsilon''}{\varepsilon'^2 + \varepsilon''^2} = M' + jM'' \quad (1)$$

where ε', M' are the real and ε'', M'' the imaginary parts of dielectric permittivity and electric modulus,

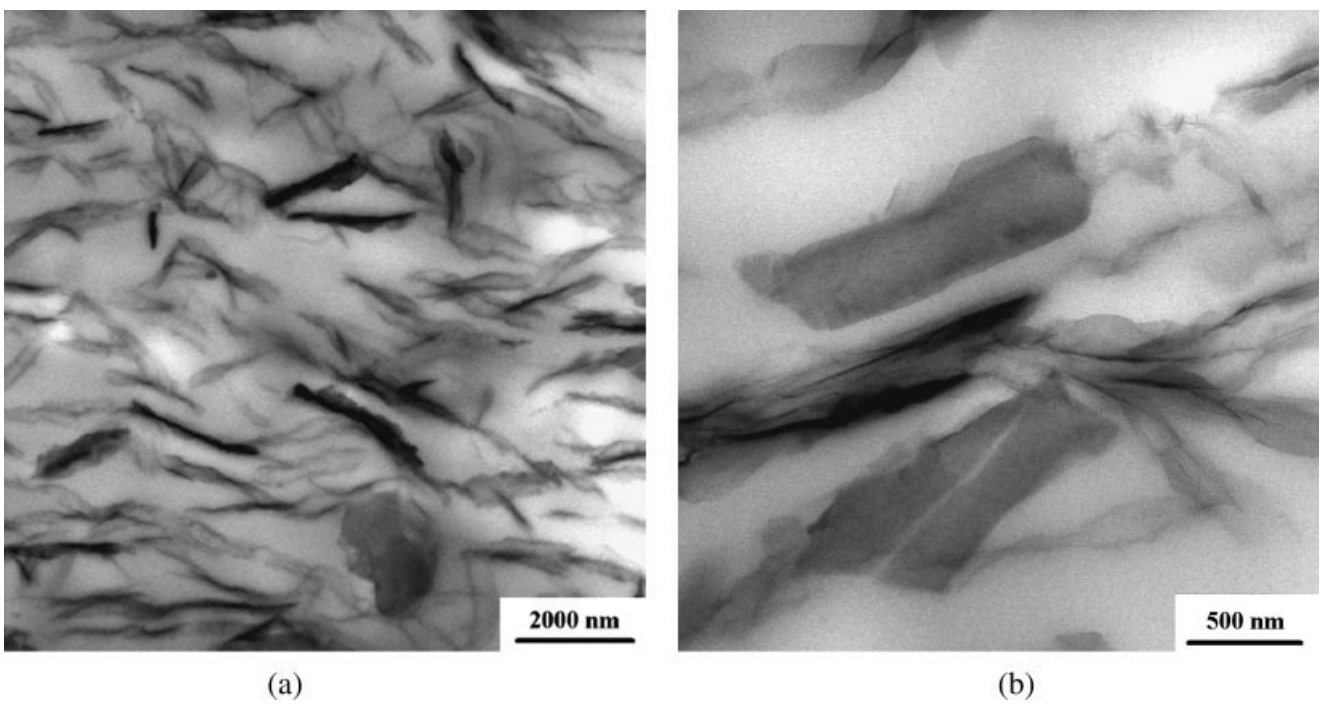

Figure 1 TEM images at two magnifications for the PUR + 10 phr LS nanocomposite.

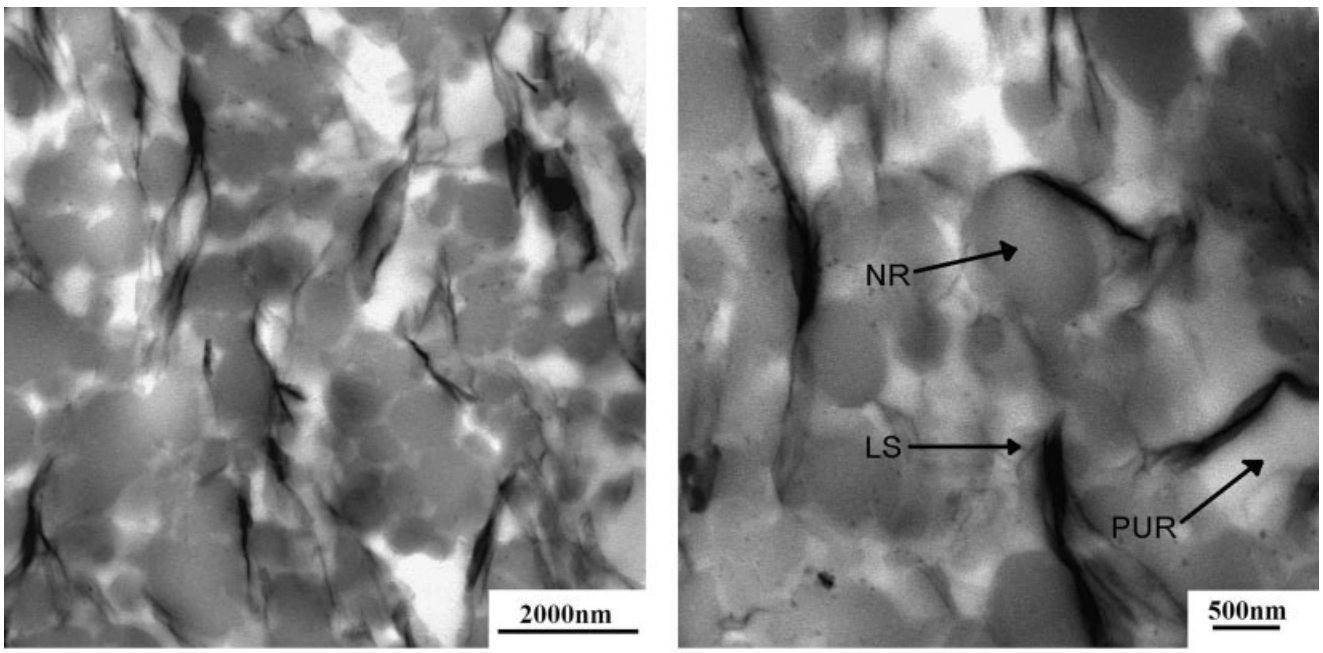

Figure 2 TEM images at two magnifications for the PUR/NR + 10 phr LS nanocomposite. *Note*: the vulcanized more or less spherical NR particles are well resolved.

respectively. Electric modulus formalism offers some advantages in the interpretation of bulk relaxation phenomena in complex systems.[11–13] Because of its own definition, large variation in the permittivity and loss at low frequencies is minimized. Further, difficulties occurring from the electrode nature and electrode/specimen contact, and conduction effects owing to the injection of space charges and absorbed impurity can be neglected.[11–13]

Figure 4 depicts the dielectric response of the employed rubber matrices at room temperature. The highest values for both real and imaginary part of electric modulus are recorded for NR, implying via Eq. (1) that NR is a material of low dielectric permittivity and loss. Considering the variation of the real part of electric modulus (M') as a function of frequency [Fig. 4(a)] one can notice a common feature for all three specimens: the onset of a step-like transition from low to high values of M' at a given frequency. NR exhibits only one transition in the low-frequency edge, while in the spectra of PUR and PUR/NR samples three distinct transitions have been recorded (indicated by arrows). These transitions imply the presence of relaxation processes and should be accompanied by relative loss peaks when plotting the imaginary part of electric modulus (M'') versus frequency [Fig. 4(b)]. The electric modulus loss index (M'') for NR attains high values in the low-frequency range and only its course suggests that here a peak may be present. In pure NR, the absence of a reinforcing phase excludes all interfacial relaxation phenomena. As NR has no polar side

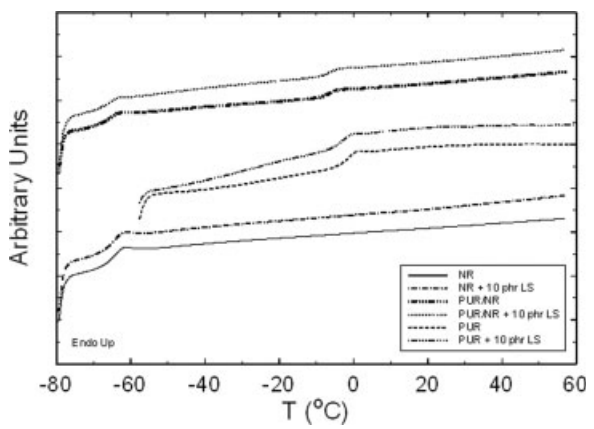

Figure 3 DSC thermographs for all the examined systems.

TABLE II
Glass Transition Temperatures (T_g) and Conductivity (σ)[a] of all the Examined Systems

	T_g (°C)	σ (S cm^{-1})
NR	−64.1	8.56×10^{-16}
NR + 10 phr LS	−64	4.71×10^{-15}
PUR	−1.1	1.11×10^{-13}
PUR + 10 phr LS	−1.8	1.90×10^{-12}
PUR/NR	−6.4/−65.0	3.56×10^{-13}
PUR/NR + 10 phr LS	−6.6/−65.4	5.28×10^{-14}

[a] Conductivity values correspond to the lowest measured frequency of 10^{-3} Hz.

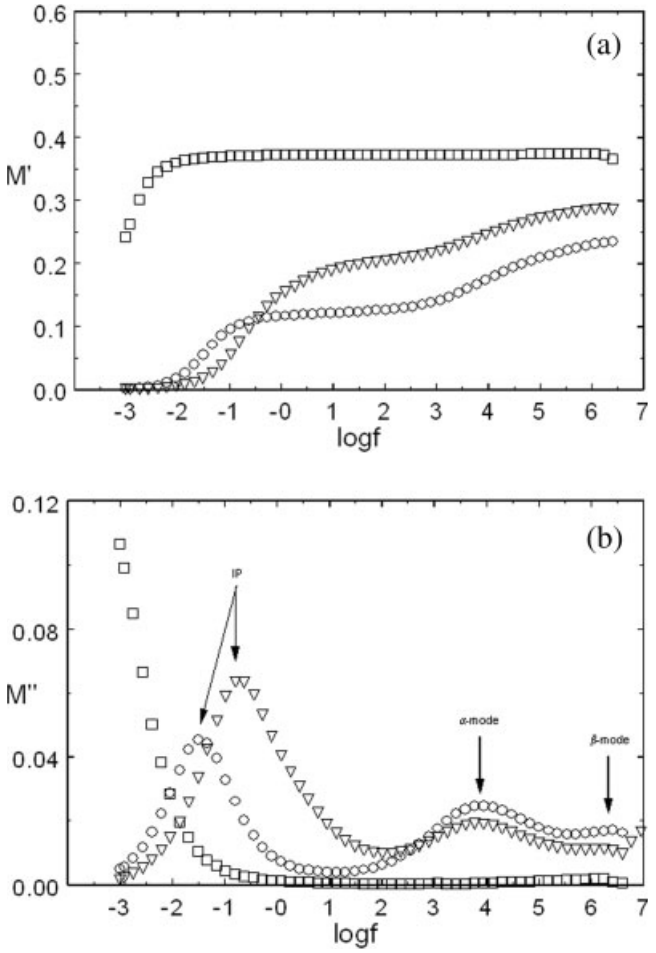

Figure 4 Real (a) and imaginary (b) part of electric modulus for the (□) NR, (○) PUR, and (▽) PUR/NR systems.

groups the recorded electrical relaxation must be attributed to the glass/rubber transition (namely α-relaxation). However, the corresponding loss peak is not completely recorded due to the low value of the glass transition temperature, $T_g = -64.1°C$ (cf. Fig. 3). Full recording of the α-relaxation peak requires measuring at lower frequencies or higher temperatures. On the other hand, in the PUR and PUR/NR spectra three relaxation modes appear. From the low-frequency edge to the high one, the relaxation mechanisms are attributed to interfacial polarization (IP) or Maxwell–Wagner–Sillars (MWS) effect, glass/rubber transition (α-mode), and polar side groups motion (β-mode). IP has been detected in the dielectric spectrum of PUR systems in previous studies.[14,15] Its occurrence was ascribed to ionic polarization at the interface of hard and soft regions and to variations of morphology between amorphous and crystalline segments. The corresponding peak of the PUR/NR blend is formed at higher frequencies; it is broader and acquires an increased maximum value of modulus loss index. Since PUR and NR are not compatible,[5] it is possible that the observed changes are introduced by the presence of the two polymer phases within the same system. Loss peak position of α-mode for both the pure PUR sample and the PUR part of the blend is recorded at the same frequency, while the glass/rubber transition of the NR part of the blend appears to be absent in the examined frequency range. Finally, at higher frequencies a faster relaxation process occurs. This can be assigned to the motion of PUR polar side groups imposed by the applied electric field.

The real (M') and the imaginary (M'') parts of electric modulus as a function of frequency for the LS-reinforced specimens are shown in Figure 5. Just like NR, the NR + 10 phr LS specimen attains higher values and in the low-frequency region exhibits a step-like transition from low to high values of (M'). However, this transition appears to be broader and less sharp than for the pure NR. The existence of a second phase (viz., LS) in the NR + 10 phr LS nanocomposite is expected to give rise to IP or MWS effect. Plotting the imaginary part of electric modulus (M'') as a function of frequency [Fig. 5(b)] results

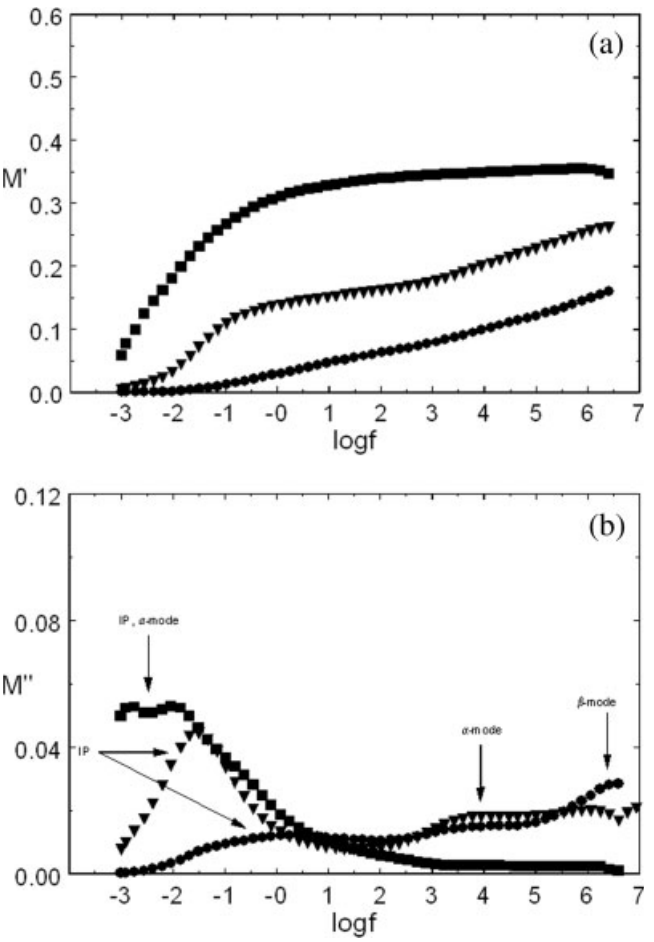

Figure 5 Real (a) and imaginary (b) part of electric modulus for the (■) NR + 10 phr LS, (●) PUR + 10 phr LS, and (▼) PUR/NR + 10 phr LS nanocomposites.

in the formation of a broad or double peak in the low-frequency range. Ascribing the recorded loss index trace to specific relaxation process or processes cannot be carried out unambiguously. It is reasonable to suggest that the presence of the LS filler shifts the glass transition temperature to somewhat higher value, and at the same time, facilitates the formation of large dipoles at the interface of the system. Intercalation of polymer molecules within parallel solid layers has been considered[7,16–19] as responsible for changing the dynamics of the polymer chains. Segmental relaxation of confined chains is faster than that of the bulk polymer.[7,18,19] Isolated polymer molecules within the galleries are not involved in cooperative molecular motions. This results in higher relaxation rate or lower glass transition temperature. Considering that both processes (IP and chain relaxation) are slow, it is thus possible to resolve them in the same, relative narrow, frequency range. In that case, the two modes are overlying to each other and their deconvolution requires the investigation of temperature effect upon the recorded dielectric response.

On the other hand the PUR/NR + 10 phr LS sample is characterized by the presence of, at least two transitions, while the PUR + 10 phr LS system exhibit a rather complex behavior. Plotting the imaginary part of electric modulus (M'') as a function of frequency [Fig. 5(b)] indicates the corresponding peaks. The presence of PUR α-relaxation mode is evident in both systems and it is recorded in the same frequency region as for the pure PUR. At higher frequencies the β-relaxation process is detected. In the low-frequency range, the PUR/NR + 10 phr LS spectrum resembles to the response of PUR and thus the corresponding peaks should be originated by the same physical process. Shape, intensity, and maximum locus of both peaks are almost identical and thus they are attributed to IP.

The situation becomes different in the case of the PUR + 10 phr LS sample, where its low-frequency peak is very broad, shifted to higher frequency and its intensity is significantly lower. IP or MWS effect is observed in heterogeneous systems because of the accumulation of mobile charges at the constituents interface. One of the characteristics of MWS effect is the high values of dielectric permittivity in the low-frequency range, which vanish rapidly with frequency.[11–13] Furthermore, increasing the heterogeneity of the system yields enhanced values of the dielectric loss index (ε''). At this point, it should be noted that expressing the same data in the electric modulus formalism via Eq. (1) will provide reducing values of modulus loss index (M'') with the increase of the intensity of IP. So, it is reasonable to suggest that the lower values of the modulus loss index (M'') is a strong indication for the existence of pronounced interfacial phenomena in the PUR + 10 phr LS system. In addition, the broadness of the corresponding peak should be related to interactions occurring between the constituents of the system. It is evident from Figures 4 and 5 that the dielectric response of the PUR + 10 phr LS system, especially in the low-frequency range, is essentially different from the corresponding behavior of all the other nanocomposites. This suggests significant differences in their morphologies. Recalling the XRD data for the PUR + 10 phr LS nanocomposite, there are two intercalated LS populations (cf. Table I). Thus, it is reasonable to suggest that these two geometries of the intercalated entities contribute to interfacial relaxation phenomena with slightly different dynamics or relaxation times. Keeping also in mind that a possible partial exfoliation, produces isolated silicate layers causing additional interfaces in the system. The formation of dipoles at the interfaces, with varying geometrical characteristics, of the PUR + 10 phr LS nanocomposite gives rise to relaxation processes. Such differences in the geometry are reflected by the rate of dielectric response or relaxation time of each contributing entity. Superposition of all interfacial effects leads to the formation of the broad peak, whose maximum locus is recorded at a frequency higher than that of the pure PUR. This shift intimates a faster overall relaxation process (shorter relaxation time) caused by the induction of, reduced in size, dipoles at the intercalated (or exfoliated) LS interfaces. Resolving the complex form of dielectric spectrum and evaluation of the relaxation time of each process requires measuring the same effects with temperature as a parameter, which will be the subject of a forthcoming study. Loss peak positions for the α and β relaxation modes of the PUR seem not be influenced by the presence of LS filler. In a previous study, concerning PUR latex/water dispersible boehmite alumina nanocomposites, it was found that their dielectric spectrum displays three distinct and well-separated relaxation processes (IP, α-mode, and β-mode).[20] This is an indirect support for the above argumentations. Hence since PUR-based nanocomposites exhibit a complex dielectric response only in the presence of LS.

For comparison, the dielectric behavior of all tested systems is given in the Cole–Cole plot (cf. Fig. 6). The suppressed semicircles correspond to the relaxation processes occurring in each of the specimens. Variation of the semicircles radius as well as the position and amplitude of the recorded processes, express the influence of composition and reinforcement. With the exception of the NR sample, the traces of all other specimens are passing from the origin of the $M'' = f(M')$ diagram indicating that no other relaxation process is present in their dielectric spectra at lower frequencies. It is noteworthy that

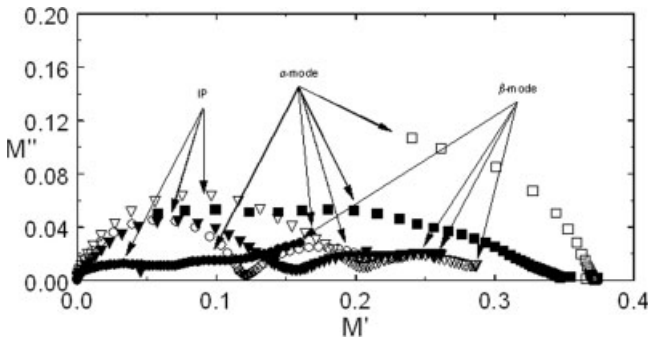

Figure 6 Cole–Cole plot of all the examined systems: (□) NR, (○) PUR, (▽) PUR/NR, (■) NR + 10 phr LS, (●) PUR + 10 phr LS, and (▼) PUR/NR + 10 phr LS.

conductivity values for all specimens was low (Table II), and thus no considerable contribution to the electrical response of the systems is expected to subsist. Conductivity relaxation is a slow electrical process characterized by enhanced relaxation time, compared with that of IP. The coincidence of the beginning of the semicircles with the origin of the diagram provides secondary support to the conclusion that the slower recorded process corresponds to IP. The uncompleted semicircle trace of NR is in accordance with its low glass transition temperature.

CONCLUSIONS

The morphology-dependent dielectric response of NR-, PUR-, and PUR/NR-based nanocomposites, prepared by adding a pristine synthetic LS (sodium fluorohectorite) in 10 phr, following the latex compounding route, was investigated in the present study. From the experimental data the following conclusions can be drawn. IP is detected in the low-frequency region of the dielectric spectra for all nanocomposites. In the high-frequency edge the PUR-containing systems exhibit β-relaxation mode resulting from the motion of polar side groups. LS appears to be more compatible and thus better intercalated by the PUR than by the NR. NR is a material of low dielectric permittivity and loss, and its α-mode is not fully recorded due to its low glass transition temperature. The presence of LS as reinforcement modifies its performance due to the occurrence of IP and possible variation of the dynamics of confined/intercalated polymer chains. The dielectric spectrum of PUR/NR + 10 phr LS exhibits three relaxation processes attributed to IP, glass/rubber transition of PUR, and β-mode. The complex form of the dielectric spectrum of the PUR + 10 phr LS was attributed to the superposition of interfacial relaxation phenomena considering two intercalated populations of LS in PUR. Finally, the α and β relaxation modes of PUR were less significantly affected by the presence of LS.

References

1. Tanaka, T.; Montanari, G. C.; Mülhaupt, R. IEEE Trans Dielectric Electr Insulat 2004, 11, 763.
2. Montanari, G. C.; Fabiani D.; Palmieri, F.; Kaempfer, D.; Thomann, R.; Mülhaupt, R. IEEE IEEE Trans Dielectric Electr Insulat 2004, 11, 754.
3. Karger-Kocsis, J.; Wu, C.-M. Polym Eng Sci 2004, 44, 1083.
4. Vaia, R. A.; Sauer, B. B.; Tse, O. K.; Giannelis, P. J Polym Sci Part B: Polym Phys 1997, 35, 59.
5. Varghese, S.; Gatos, K. G.; Apostolov, A. A.; Karger-Kocsis, J. J Appl Polym Sci 2004, 92, 543.
6. Utracki, L. A.; Kamal, M. R. Arab J Sci Eng 2002, 27, 43.
7. Elmahdy, M. M.; Chrissopoulou, K.; Afratis, A.; Floudas, G.; Anastasiadis, S. H. Macromolecules 2006, 39, 5170.
8. Lee, H.-T.; Lin, L.-H Macromolecules 2006, 39, 6133.
9. Riande, E.; Díaz-Calleja, R. In Electrical Properties of Polymers; Marcel Dekker: New York, 2004; Chapters 8 and 14.
10. Kremer, F.; Schönhals, A. In Broadband Dielectric Spectroscopy; Kremer, F., Schönhals A., Eds.; Springer: Berlin, 2003; p. 35, 395.
11. Tsangaris, G. M.; Psarras, G. C.; Kouloumbi, N. J Mater Sci 1998, 33, 2027.
12. Psarras, G. C.; Manolakaki, E.; Tsangaris, G. M. Composites A 2002, 33, 375.
13. Psarras, G. C.; Manolakaki, E.; Tsangaris, G. M. Composites A 2003, 34, 1187.
14. Pissis, P.; Kanapitsas, A.; Savelyev, Y. V.; Akhranovich, E. R.; Privalko, E. G. Polymer 1998, 39, 3431.
15. Korzhenko, A.; Tabellout, M.; Emery, J. R. Polymer 1999, 40, 7187.
16. Lu, H.; Nutt, S. Macromolecules 2003, 36, 4010.
17. Page, K. A.; Adachi, K. Polymer 2006, 47, 6406.
18. Lee, Y.-H.; Bur, A. J.; Roth, S. C.; Start, P. R. Macromolecules 2005, 38, 3828.
19. Anastasiadis, S. H.; Karatasos, K.; Vlachos, G.; Manias, E.; Giannelis, E. P. Phys Rev Lett 2000, 84, 915.
20. Gatos, K. G.; Martínez Alcázar, J. G.; Psarras, G C.; Thomann, R.; Karger-Kocsis, J. Compos Sci Technol 2007, 67, 157.